STRUCTURE OF SOLAR FACULAE

[1,2]Solov'ev A.A. [1]Kirichek E.A.

[1]*Central astronomical observatory of Russian Academy of Science, S-Petersburg, Russia*

[2]*Kalmyk State University, Elista, Russia*

solov@gaoran.ru

Abstract

In solar facular regions (plages) three distinct classes of magnetic features are observed: small-scale flux tubes, knots, and pores. Small flux tubes have granular scales; they are in constant motion and can well be simulated numerically according to the concept of magneto-convection. On this dynamic background one observes quite stable, long-lived and bright objects called facular knots, with a diameter of 3-8 Mm and fine (less than 1 Mm) inner filamentary structure. Their magnetic field strength varies in the range from 250 to 1200 G. Our present article considers only these active formations. The stationary MHD problem is solved and analytical formulae are derived for calculation the pressure, density, temperature, and Alfven Mach number in the studied configuration from the corresponding magnetic field structure. The facular knot is modeled in a hydrostatic atmosphere defined by the Avrett & Loeser model (2008) and is surrounded by a weak (2 G) external field corresponding to the average global magnetic field strength on the solar surface. The constructed 3D analytical model presents the facular knot as a magnetic "fountain" with numerous slender fibrils and allows solving the following tasks: 1. Calculation of temperature profiles of the knot at any height of the atmosphere; 2. Description of ring brightening and fine azimuthal fibril structure observed in plages at high spatial resolution; 3. New interpretation of Center-to-Limb Variation problem that fits well with the observational data.

Key words: Sun; chromosphere; faculae; magnetic field; temperature

1. Introduction

Solar faculae represent, second after sunspots, significant and prominent manifestation of solar activity. Despite the fact that facula is marginally luminous in

comparison to the **quiet** photosphere nevertheless the contribution of faculae as a whole cannot be ignored. This can be ascertained by considering that the Total Solar Irradiance is higher (by 0.1%) at the peak of the sunspot activity than at the minimum, i.e. the increased luminosity of the faculae overlaps the decrease in the total luminosity of the Sun, caused by the appearance of dark sunspots. This is one of the reasons why great attention has been paid to the study of faculae in solar physics. Faculae, like sunspots, are magnetic in nature, although their magnetic fields are much weaker in comparison to that of spots. Obviously, for this reason, the appearance of faculae in active regions precedes and succeeds the formation of sunspots. It is generally accepted (Title et al., 1992) that there are three different classes of magnetic structures in the facular regions: 1. Small-scale magnetic elements; 2. Facular knots and 3. Pores. The first category has "granular" scales (Title and Berger, 1996; De Pontieu et al, 2006; Steiner, 2005; Berger et al, 2007): diameter of 0.5-1 angular seconds, lifetime of about 5-10-15 minutes, and magnetic field strength close to the equipartition level (150-250 Gs). These small, short lived elements are very dynamic as they are in constant motion and their low brightness is due to the interaction with magnetic field of convective granules which results in a slight compression leading to increased luminosity and consequent magnetic structuring of plasma. These structures manifest themselves through "the dense forest" of more transparent magnetic flux tubes surrounding them (Berger et al, 2007; Topka et al, 1997). The physical nature of these elements is well simulated numerically in the framework of magneto-convection (Keller et al., 2004).

Against this changing background, however, separate, less mobile, more stable, larger and long-lived facular formations (facular knots) that live up to a day or more are observed in plages. So, the single facular formation with the angular size about 4-10 arcsec, magnetic field strength about 900 G and lifetime more than 13 hours was studied in detail by (Kolotkov et al., 2017) for the detection of long-term oscillations with periods of more than an hour. Apparently, these objects are located at the junctions of several supergranular convection cells. In these cells radial-horizontal

plasma flows concentrate to several dozens of magnetic facular elements, which look like separate magnetic flux tubes or bundles, into inter-supergranular lanes, raking them as a result of the frozen field in plasma to the edges of the cells (Mehltretter,1974). The plasma flows and reduced gas pressure in the intergranular lanes provide the required stabilizing effect for a prolonged existence of the facular knots. Therefore, these structures can be considered as stable formations, capable to oscillate as integral objects near the equilibrium position. Although on the whole the knots have an increased brightness, they exhibit a central dip in temperature profile (like the Wilson depression in sunspots) and in this sense they already approach pores **which are** small dark sunspots without penumbras.

In this work, we will investigate only such relatively stable, large and long-lived bright photospheric-chromospheric magnetic formations which are termed as the facular knots. The gas temperature in the facular knot on the average is few hundred degrees Kelvin higher than the temperature of the surrounding atmosphere, and the temperature contrast between the individual bright elements inside the body of facular knot does not, probably, exceed 100-200K. At high angular resolutions (New Swedish 1-m Telescope), the facular fields in the photosphere are observed to possess besides the central temperature dip a regular concentric segmental brightening (Lites et al., 2004, Berger et al., 2007). Explanation of the nature of these specific temperature variations is one of the tasks of the present model. Recently (Jafarzadeh et al, 2017), when observing the low chromosphere at altitudes of the temperature minimum, observed a very fine structure in the form of "slender CA II H fibrils mapping magnetic fields". A similar result was earlier obtained in (Pietarila et al. 2009) by observations in CA II K line. This remarkable phenomenon of very fine structure of chromospheric fibrils also requires its own description and explanation.

There are various kinds of wave and oscillatory processes that are observed in the facular fields. Roughly speaking these oscillations can be divided into two classes of different physical nature. The most studied are short-period oscillations with periods from 3-5 and 10-15 minutes (see, for example, Baltasar,1990; Chelpanov, Kobanov & Kolobov, 2015 and many others). They are usually interpreted as manifestations of

acoustic and MHD waves running along magnetic flux tubes in the faculae where these flux tubes play the role of resonators or waveguides. Many works have been devoted to the study of these processes, but they practically do not shed light on actual magnetic structure of faculae. Observing these wave phenomena, one can only estimate the phase velocities of the waves in order of magnitude and, accordingly, obtain the averaged order estimates of the magnetic field intensity and the plasma density. However, recently there have been reports that long-period oscillations with periods from 1 to 4 hours are observed in large stable faculae (Kolotkov et al., 2017; Strekalova et al., 2016). These oscillations can no longer be understood within the framework of propagating MHD wave models or within the framework of the "vortex shedding" mechanism originated due to the stream flowing outside the faculae (Nakariakov et al., 2009). Apparently, they reflect the oscillations of the faculae as a whole, as a single magnetic structure. In such oscillations, significant masses of gas are involved in the oscillatory process and therefore their periods are sufficiently large.

However, here we are not going to consider the problem of the oscillatory properties of faculae (it would require a separate study), but will concentrate only on the construction of their 3D steady state analytical MHD model.

One of the first physical models of the faculae was the "hot wall" model (Spruit, 1976). It represents the faculae as a vertical magnetic flux tube penetrating deep into the photosphere and even into the upper part of convective zone. It is assumed that the plasma density in such a tube is sharply reduced, and thus a deep Wilson depression is created which, if viewed from the side, allows us to see through the transparent tube of the faculae the hot layers of the photosphere and the convective zone - hot walls. However, this simply overlooks the fact that when such a flux tube is observed on the limb, the observer's line of sight passes at right angles to the axis of the radially oriented facular tube, and its low layers, its hot walls, are simply not visible in this position. It turns out that, according to this model, faculae cannot be observed on the limb in principle. However, observations show the opposite picture: faculae are best seen on the limb! This drawback of the model was noted in many works (Libbrecht

& Kuhn, 1984; Shatten et al.,1986; Wang & Zirin,1987). Nevertheless, observers still refer to this model: Quintero et al. (2016). Kostik & Khomenko (2016), analyzing the causes of the observed brightness of facular tubes, likewise come to the conclusion that " facular regions appear bright not only because of the Wilson depression in magnetic structures, but also owing to real heating". Earlier, the same opinion has been expressed in (Chapman & Klabunde,1982).

The other model is "hillock and cloud model" for faculae (Shatten et al., 1986). It tries to describe faculae as objects not related to specific magnetic structure but possessing enhanced brightness in the vicinities of sunspots mainly due to the uplifting of hot sub-photospheric plasma which is otherwise entrapped because of the large magnetic fields near the sunspot. This vertical transfer of sub-photospheric hot plasma according to the authors is assumed to take place along different magnetic flux tubes with arbitrary parameters, being produced by unknown physical mechanisms, and results in the formation of hot clouds which are actually observed by the observers as faculae. This model according to our opinion doesn't represent the real physical nature of faculae and therefore can be mentioned for purely historical reasons.

2.1. Stationary MHD and the governing equations

System of equations of ideal MHD in the steady case has the following form:

$$\rho\left(\mathbf{V}\cdot\nabla\right)\mathbf{V} = -\nabla P + \left(4\pi\right)^{-1}\left[curl\mathbf{B}\times\mathbf{B}\right] + \rho\mathbf{g}, \qquad (1)$$

$$div\left(\rho\mathbf{V}\right) = 0, \qquad (2)$$

$$div\mathbf{B} = 0, \qquad (3)$$

$$P = \rho\Re T\mu^{-1}. \qquad (4)$$

Here $\mathbf{B}$ is magnetic field vector, $\mathbf{V}$ is flow velocity vector of the fluid, P, ρ, T, μ are pressure, density, temperature and average molar mass of the gas respectively.

The energy transport equation which has a very complicated form for solar plasma is left undetermined. Exact analytical solutions to the problems of heat transfer and energy dissipation in active solar elements like sunspots, faculae, prominences, coronal loops and etc. are now almost impossible not only because of complicated

geometry, spatial inhomogeneity and tremendous difficulty in 3D radiative transfer calculations in the continuum and in the spectral lines. We likewise have further difficulties because of our inability to reliably evaluate the contribution of MHD wave dissipation and electric current heating (Joule heating) to the energy balance of the given magnetic structure under study.

Our approach to the modeling of active solar elements is as follows: equations (1)-(4) allow to determine the pressure, density, temperature and velocity of the plasma configuration required for its steady existence in the case when the magnetic structure of the element is considered to be known. The stationary distributions of temperature and density derived for a given magnetic structure should answer maximally the observational properties of the modeled object.

When such a result is obtained we can be sure that the magnetic structure of the object was chosen correctly. At the same time, we must be prepared to explain the physical reasons for why the theoretically obtained from the balance of forces temperatures turned out to be such that they are observed in reality. Evidently, the correspondence of the observed and theoretically found temperature distributions should be explained by a specific heat transfer mechanism in the given configuration. For example, in the case of a sunspot, all models must present considerable low temperature of the umbra with respect to the surrounding photosphere because the strong vertical magnetic fields inhibit the convective motion of plasma in sunspots. Likewise, when the equilibrium model of the solar filaments or prominences gives the very cool plasma in their dense bodies, one can explain the low temperature derived from the steady state condition as a result of fast cooling of the gas due to high irradiance of dense plasma in the coronal conditions.

Most probably faculae, fibrils and floccules share one and the same magnetic flux tube structure. Also it is quite possible that these structures are heated by wave dissipative processes and/or by joule heating mechanism in rarefied plasma as it occurs in the solar corona. Unlike corona which has very low density and therefore very high temperature, the chromospheric structures like fibrils, floccules and photospheric structures like faculae are not very hot because of corresponding high chromospheric densities in comparison with corona.

2.1. Boundary conditions of the problem

Facular knots are regarded as sufficiently solitary magnetic structures and therefore their magnetic field at large heights and at large radial distances from the center of the facular field should attain some background value.

The demarcation boundary at the bottom of the facular structure is defined as the depth at which the average magnetic pressure in the magnetic flux tube is comparable to the dynamic pressure of convective turbulent pulsations in the photosphere: $\left\langle (8\pi)^{-1} B^2 \right\rangle = 0.5\rho(Vturb)^2$. At this bottom boundary the radial profiles of pressure and temperature should have the typical form where the central region is a bit lower than the surroundings, and at large distances from the center, the profiles approach photospheric values.

At the periphery of this magnetic structure, the radial component of magnetic field vector approaches zero and the balance of total pressures on either sides of the object is attained as it was demonstrated in the work (Solov'ev & Kirichek, 2015) which studied the equilibrium of vertical magnetic flux tubes in the solar atmosphere. However, as our calculations show, there is no need to attribute an abrupt sideward boundary to the facular knot in our model because the described parameters steadily approach the background values as we move away from the center of the object.

2.2. Derivation of the governing equation

According to stationary ideal MHD, the plasma flows along the magnetic lines of force:

$$\mathbf{V} = M_A \frac{\mathbf{B}}{\sqrt{4\pi\rho}}, \tag{5}$$

where $M_A = \dfrac{V}{V_A}$ is Alfven Mach number, the ratio of the plasma fluid velocity and the corresponding Alfven velocity. From the equations (2), (3) and (5) it follows that:

$$\mathbf{B} \cdot \nabla \left(M_A \sqrt{4\pi\rho} \right) = 0, \tag{6}$$

i.e. the factor $M_A \sqrt{\rho}$ doesn't change along the magnetic field line but can vary arbitrarily as we move from one field line to an another.

We assume that the plasma flow inside the facular knot is not very strong, Alfven Mach number does not exceed unity, and the flow remains sub-alvenic. Likewise, the external plasma flow with respect to the facular knot remains sub-alfvenic. The super-convective converging flow is added up to the hydrostatic pressure $P_{ex}(z)$ of the external medium at the photospheric level as a very small dynamic component $0.5\rho_{ex}(z)V_{super}^2$, where V_{super} is the velocity of horizontal flow in super-granulation cells. The height profile for this velocity field is unknown and it is only possible to give an order of magnitude value: $V_{super} \approx 0.3 \div 0.5 km/s$. The Alfven velocity in the chromosphere with a magnetic field strength of about 10 G or more exceeds 10 km/s and therefore Alfven Mach number for external layers of the facular knot is $M_A^2 < 1$.

The magnitude of the plasma flow velocity inside the knot doesn't exceed $1.0 \, km/s$ (Quintero et al., 2016). The same estimation is quite satisfactory for polar faculae (Okunev & Kneer, 2004) and therefore we can safely assume that the flow field of gas inside these knots is sub-alfvenic: $M_A < 1$.

We rearrange the L.H.S of the equation (1), using the condition (5):

$$\rho(\mathbf{V}\nabla)\mathbf{V} \equiv \rho\left(\frac{1}{2}\nabla V^2 + [curl\mathbf{V} \times \mathbf{V}]\right) =$$
$$= \rho\left\{\frac{1}{2}\nabla\left(\frac{M_A^2}{4\pi\rho}B^2\right) + \frac{M_A^2}{4\pi\rho}[curl\mathbf{B} \times \mathbf{B}] + \frac{M_A}{\sqrt{4\pi\rho}}\left[\left[\nabla(\frac{M_A}{\sqrt{4\pi\rho}}) \times \mathbf{B}\right] \times \mathbf{B}\right]\right\}. \qquad (7)$$

We use the respective vector identity and the relation (6) to get the following equation:

$$\rho(\mathbf{V}\nabla)\mathbf{V} = \rho\left\{\frac{M_A^2}{4\pi\rho}\left(\frac{1}{2}\nabla B^2 + [curl\mathbf{B} \times \mathbf{B}]\right) + \frac{M_A}{\sqrt{4\pi\rho}}\mathbf{B}\cdot\left(\mathbf{B}\cdot\nabla\left(\frac{M_A}{\sqrt{4\pi\rho}}\right)\right)\right\}. \qquad (8)$$

We transform the last term in the R.H.S of equation (8) using again the condition (6) to obtain the following equation for the steady state of the system:

$$M_A^2(\mathbf{B}\cdot\nabla)\mathbf{B} + \mathbf{B}(\mathbf{B}\cdot\nabla M_A^2) = -4\pi\,\nabla P + [curl\mathbf{B} \times \mathbf{B}] + 4\pi\,\rho\mathbf{g}. \qquad (9)$$

At last, by representing the magnetic part of Lorenz force as

$[curl\mathbf{B} \times \mathbf{B}] = -\frac{1}{2}\nabla B^2 + \mathbf{B}(\nabla\mathbf{B})$, we rewrite (9) in the form (Solov'ev & Kirichek, 2016),

which constitutes the base our present research:

$$(1-M_A^2)(\mathbf{B}\cdot\nabla)\mathbf{B} + \mathbf{B}(\mathbf{B}\cdot\nabla(1-M_A^2)) = 4\pi\nabla\,(P + \frac{B^2}{8\pi}) - 4\pi\,\rho\mathbf{g}. \qquad (10)$$

The idea behind our approach is based upon the experimental observations of the long lived and stable active elements such as sunspots, pores, facular knot, chromospheric filaments (fibrils) and prominences, we construct the magnetic configuration of these objects up to the accuracy of few arbitrary functions and then solve the stationary MHD problem for these magnetic structures and finally obtain pressure, density and Alfven Mach number from the three components of equation (10). Later, the obtained pressure and density distributions are used in accordance with the ideal gas equation to find the respective temperature distribution. In this way for every given

configuration of the magnetic field **B(r)** we can calculate all the required physical parameters P, ρ, T, M_A for the stationary existence of this configuration. This allows us to compare the theoretically obtained results with the observed data. The arbitrariness in the expression for the magnetic field allows us to freely choose the most relevant function that best fits the observed data. The same approach was used for modeling the sunspot (Solov'ev & Kirichek, 2016).

3. Magnetic structure of steady facular configuration

We shall assume that the magnetic field of our configuration under study is not twisted i.e. the field has only two independent components but both of them are dependent on all three coordinates in the cylindrical system (r, φ, z):

$$\mathbf{B} = \{B_r(r, \varphi, z)\mathbf{e}_r, 0 \cdot \mathbf{e}_\varphi, B_z(r, \varphi, z)\mathbf{e}_z\} \qquad (11)$$

The z-axis is directed upward along the major axis of the cylinder and the gravitational force is represented by: $\rho\mathbf{g} = -\rho g\mathbf{e_z}$. The azimuthal component of the equilibrium equation (10) for the magnetic field of the type (11), with $B_\varphi = 0$, reduces to a following simple form:

$$\frac{\partial}{\partial \varphi}(P + \frac{B^2}{8\pi}) = 0. \qquad (12)$$

From the above expression we get the important formula for the pressure balance as:

$$P(r, \varphi, z) + \frac{B^2(r, \varphi, z)}{8\pi} = \Pi(r, z). \qquad (13)$$

The function $\Pi(r, z)$ can be clearly interpreted as the total (Gas + Magnetic) pressure which doesn't depend on the cylindrical angular coordinate but preserves the dependence on r and z. Far away from the knot it takes the following form:

$$\Pi(\infty, z) = \frac{B_{ex}^2(z)}{8\pi} + P_{ex}(z), \qquad (14)$$

where B_{ex} is the external magnetic field strength with respect to the given magnetic configuration, and $P_{ex}(z)$ is the gas pressure out of the knot. In case of small B_{ex} we

have $\Pi(\infty, z) = P_{ex}(z)$. Though there is small-scale turbulence in the photosphere we can fairly assume that it is very close to the hydrostatic state:

$$\frac{\partial P_{ex}(z)}{\partial z} = -g\rho_{ex}(z). \tag{15}$$

We now write down equations for two other components in the equation (10) by substituting expression (13) in the R.H.S.

$$\frac{(1-M_A^2)}{4\pi}\left(B_z\frac{\partial B_z}{\partial z} + B_r\frac{\partial B_z}{\partial r}\right) + \frac{B_z}{4\pi}\left(B_z\frac{\partial(1-M_A^2)}{\partial z} + B_r\frac{\partial(1-M_A^2)}{\partial r}\right) =$$
$$= g\rho(r,\varphi,z) + \frac{\partial\Pi(r,z)}{\partial z}, \tag{16}$$

$$\frac{(1-M_A^2)}{4\pi}\left(B_z\frac{\partial B_r}{\partial z} + B_r\frac{\partial B_r}{\partial r}\right) + \frac{B_r}{4\pi}\left(B_z\frac{\partial(1-M_A^2)}{\partial z} + B_r\frac{\partial(1-M_A^2)}{\partial r}\right) = \frac{\partial\Pi(r,z)}{\partial r}. \tag{17}$$

Now we determine the components of the magnetic field with the help of the magnetic flux function. Equation (3) in terms of cylindrical coordinates has the form:

$$\frac{\partial B_z}{\partial z} + \frac{1}{r}\frac{\partial}{\partial r}rB_r = 0, \tag{18}$$

It follows that the longitudinal and radial fields can be expressed in terms of the function $A(r,z) = \int_0^r b_z r dr$ and some arbitrary dimensionless function of the magnetic flux and the angular coordinate $F(A,\varphi)$:

$$B_z(r,\varphi,z) \equiv B_0 F(A,\varphi)\, b_z(r,z); \quad b_z(r,z) = \frac{1}{r}\frac{\partial A(r,z)}{\partial r};$$
$$B_r(r,\varphi,z) \equiv B_0 F(A,\varphi)\, b_r(r,z); \quad b_r(r,z) = -\frac{1}{r}\frac{\partial A(r,z)}{\partial z}. \tag{19}$$

B_0 is taken as the unit for the measurement of magnetic field strength. By a simple substitution of these expressions in (18), one can see that the magnetic field given by (19) is conditionally solenoidal for any arbitrary differentiable function $F(A,\varphi)$. This simple result is extremely important not only when modeling active solar formations, but also in a general physical sense. It means that in any vertical non-twisted flux tube an arbitrary angular variation of the field can be introduced! It allows, in particular, dividing the flux tube of the modeled object into many slender filaments

with the corresponding circular electric currents which could make a significant contribution to chromospheric plasma heating (along with the wave dissipation). The dependence of the function F on the angular coordinate being the arbitrarily defined, can be taken, for example, in such a simple type:

$$F^2(A,\varphi) = 1 + f(A,\varphi) = 1 + k^2 \left| A \cdot \sum_i a_i \sin(m_i\varphi) \right|, \qquad (20)$$

where $f(A,\varphi)$ is the positive oscillating function with decreasing amplitude as we move above in height because of magnetic flow A decreasing with height. In (20) a_i, m_i are some positive coefficients, k is the reciprocal height scale which was introduced here to rewrite equation (20) in a dimensionless form. The different values of m_i allow us to describe as deformed temperature profile of the knot ($m < 1$), both the fine discrete structure inside the facular knot due to the combination of radial and angular dependence in equation (20) (see Fig.1). In particular, the circular and semi-circular structures can be described which are usually observed in the facular fields at high angular resolutions (Lites et al., 2004). At large m ($m = 20, 40$) the magnetic structure with very slender fibrils can be obtained according with the observations (Jafarzadeh et al, 2017) (see Fig.1). If there is no angular dependence, than $F = 1$. By substituting expression (19) in the formulas (16) and (17) we get:

$$(1-M_A^2)F^2(A,\varphi)\frac{B_0^2}{4\pi}\left[\left(b_z\frac{\partial b_r}{\partial z}+b_r\frac{\partial b_r}{\partial r}\right)+\left(b_r b_z\frac{\partial\ln(1-M_A^2)}{\partial z}+b_r^2\frac{\partial\ln(1-M_A^2)}{\partial r}\right)\right]=\frac{\partial\Pi(r,z)}{\partial r}. \quad (21)$$

$$(1-M_A^2)F^2(A,\varphi)\frac{B_0^2}{4\pi}\left[\left(b_z\frac{\partial b_z}{\partial z}+b_r\frac{\partial b_z}{\partial r}\right)+\left(b_z^2\frac{\partial\ln(1-M_A^2)}{\partial z}+b_z b_r\frac{\partial\ln(1-M_A^2)}{\partial r}\right)\right]=$$

$$=g\rho(r,\varphi,z)+\frac{\partial\Pi(r,z)}{\partial z}. \qquad (22)$$

The R.H.S. of the expression (21) doesn't contain the angular dependence. Consequently, we must take:

$$\left[1-M_A^2(r,\varphi)\right]F^2(A,\varphi)=G(A), \qquad (23)$$

where $G(A)$ is some arbitrary function of the magnetic flow which is independent of the angular coordinate. In this case, the expression $\left[1-M_A^2(r,\varphi)\right]$ depends on A and

φ only, and therefore the logarithmic terms in the second round brackets of the L.H.S. of the equations (21) and (22) identically equal to zero due to Equation (19). As we see from (23), the negative values of $G(A)$ correspond to super-alfvenic flow $M_A^2(r,\varphi) > 1$. As it was noted above, the observations of solar plages provide no basis for such a conclusion (Quintero et al., 2016; Okunev & Kneer, 2004). Hence, we must assume that $1 > G(A) > 0$. It gives:

$$M_A^2 = 1 - \frac{G(A)}{F^2} = \frac{1 - G(A) + f}{1 + f} > 0. \tag{24}$$

In the case when $f = 0$, one has $M_A^2 = 1 - G$. As $f \gg 1$, we get $M_A^2 \to 1$. Further, for the simplicity of the model we will take $G = const > 0$. In this way equations (21), (22) take the form:

$$G\frac{B_0^2}{4\pi}\left(b_z \frac{\partial b_r}{\partial z} + b_r \frac{\partial b_r}{\partial r} \right) = \frac{\partial \Pi(r,z)}{\partial r}, \tag{25}$$

$$G\frac{B_0^2}{4\pi}\left(b_z \frac{\partial b_z}{\partial z} + b_r \frac{\partial b_z}{\partial r} \right) - \frac{\partial \Pi(r,z)}{\partial z} = g\rho(r,\varphi,z). \tag{26}$$

The L.H.S. of the equation (26) doesn't depend on the angle, consequently this dependence disappears for the distribution of plasma density which in our configuration happens to have an axially symmetric form: $\rho = \rho(r,z)$.

The expression (25) with the help of (14) is integrated with respect to r from some point infinitely distant from the knot to a point taken into the knot:

$$\Pi(r,z) = G\frac{B_0^2}{8\pi}\left[b_r^2 + 2\int_\infty^r b_z \frac{\partial b_r}{\partial z} dr \right] + P_{ex}(z) + \frac{B_{ex}^2}{8\pi}. \tag{27}$$

Substituting $\Pi(r,z)$ in (25) we get:

$$\rho(r,z) = \rho_{ex}(z) +$$
$$+ \frac{G}{g}\frac{B_0^2}{8\pi}\left[2b_r \frac{\partial b_z}{\partial r} + \frac{\partial}{\partial z}\left(b_z^2 - b_r^2 - 2\int_\infty^r b_z \frac{\partial b_r}{\partial z} dr \right) \right] - \frac{1}{8\pi}\frac{\partial B_{ex}^2}{g\partial z}. \tag{28}$$

The balance of pressures given by (27) can be rewritten as:

$$P(r,z,\varphi) = \Pi(r,z) - \frac{B^2(r,z,\varphi)}{8\pi} = P_{ex}(z) + \frac{B_{ex}^2}{8\pi} + P_m(r,z,\varphi), \tag{29}$$

where $P_m(r,z,\varphi) = G\frac{B_0^2}{8\pi}\left[b_r^2 + 2\int_\infty^r b_z\frac{\partial b_r}{\partial z}dr\right] - \frac{B^2(r,z,\varphi)}{8\pi}$ represents the deviation of gas

pressure in the system from the corresponding hydrostatic distribution caused by the magnetic field. The gas pressure (29) depends on angle due to the term $B^2(r,z,\varphi)$. The corresponding expression for the density of gas can be written as:

$$\rho(r,z) = \rho_{ex}(z) - \frac{\partial}{\partial z}\frac{B_{ex}^2}{8\pi} + \rho_m(r,z),\qquad(30)$$

where $\rho_m(r,z) = \frac{B_0^2}{8\pi}\frac{G}{g}\left[\frac{2b_r\partial b_z}{\partial r} - \frac{\partial}{\partial z}\left(b_r^2 - b_z^2 + 2\int_\infty^r\frac{b_z\partial b_r}{\partial z}dr\right)\right]$ is the deviation of density

from the hydrostatic distribution $\rho_{ex}(z)$ owing to the presence of the magnetic field in the facular knot. As we see, the density doesn't have azimuthal dependence.

In the obtained formulas the important uncertainty is constituted by the term contain-

ing $\frac{B_{ex}^2}{8\pi}$ and the derivative of it with respect to height. To consider these, we must in-

troduce an extra hypothesis. We use the simplest possible form: $B_{ex} = const = 2\,G$,

which corresponds to the global magnetic field strength at the level of the photosphe-

re (Title & Schrijver, 1998). This field varies with height by the scale of hundreds of thousands of km. At the scale of chromosphere, i.e. about 2 Mm (Avrett & Loeser, 2008), which is considered here, these changes are negligibly small and the expres-

sion for the density of the gas (30) can be considered free of the small term $\frac{1}{8\pi}\frac{\partial B_{ex}^2}{\partial z}$.

The expressions (29), (30) with the known functions $B_0 b_z(r,z)$, $B_0 b_r(r,z)$ allow us to calculate the distributions of gas pressure and gas density in the stationary facular knot. As one can notice, the exact evaluation of the magnetic force gives the equation which is considerably complex in comparison to the usually used simple equation of pressure balance $P + (8\pi)^{-1}B_z^2 = P_{ex}$ which is true only in the absence of the radial field, gas flow and angular variations of the field. Note, that the steady gas flow de-scribed by the term M_A^2 enters into the balance of pressures (29) and densities (30) both directly through the factor C, and indirectly through the function $f(A,\varphi)$ (see relation (24).

4. The structure of the magnetic field in the facular knot

For the magnetic structure of the facular knot, we can use, as an initial approximation, the solution for a potential field following Schatzman (1965):

$$B_z = B_0 J_0(kr)\exp(-kz),$$
$$B_r = B_0 J_1(kr)\exp(-kz), \qquad (31)$$

Here $J_0(kr)$, $J_1(kr)$ are the Bessel functions of zeros and first orders, B_0 is the magnetic field strength at the level of the $z = 0$ (it is the photosphere), k is the reciprocal height scale. The distributions (31) are obtained from the following magnetic flux function:

$$A(r,z) = B_0 \frac{r}{k} J_1(kr)\exp(-kz). \qquad (32)$$

The magnetic force of the potential field (31) naturally is zero; therefore this field does not produce the visible deviations in magnetic structure of facula. To get the non-potential, force configuration, we should introduce the respective corrections into the magnetic structure (31). We introduce two corrections into our model as follows: (i) angular dependence given by the function F (see formula (20) and Fig.1), and (ii) – the substitution of the exponents in (31) by the expression:

$$Z(z) = \frac{2}{\exp(kz)+1}, \qquad (33)$$

This expression describes a distorted step (analogue of the Fermi-Dirac distribution). For $z > 0$ this function approaches to $2\exp(-kz)$, and therefore the magnetic field approaches a potential form at large heights. For $z < 0$, the magnetic field in the flux tube which goes down stops to be dependent on the depth and tends to the constant $2B_0$. Thus, instead of (31) we have:
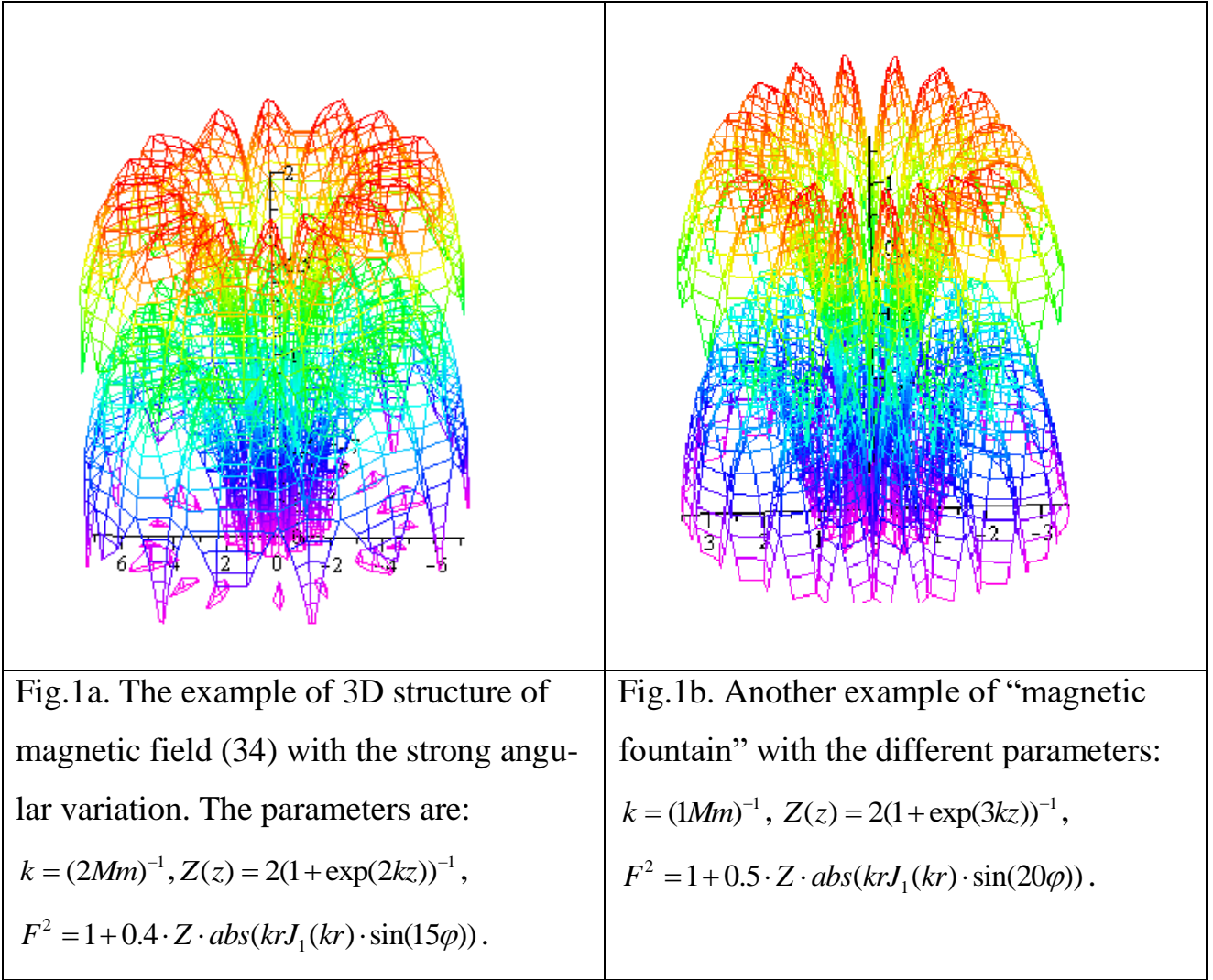
$$B_z = B_0 F(A,\varphi)Z(z)J_0(kr),$$
$$B_r = B_0 F(A,\varphi)Z(z)J_1(kr). \qquad (34)$$

In the model of quiet hydrostatic solar atmosphere of Avrett & Loeser (2008), which we use here as the environment, the level with plasma parameters: $T(0) = 6583K$, $P(0) = 1.228 \times 10^5 \; dyn/cm^2$, $\rho(0) = 2.87 \times 10^{-7} \; g/cm^3$ is taken as the base of the photosphere. The level with the temperature of 5800K, usually regarded as a typical photospheric layer, lies in this model at height of 50 km above.

Fig.1a. The example of 3D structure of magnetic field (34) with the strong angular variation. The parameters are: $k = (2Mm)^{-1}$, $Z(z) = 2(1+\exp(2kz))^{-1}$, $F^2 = 1+0.4\cdot Z\cdot abs(krJ_1(kr)\cdot\sin(15\varphi))$.	Fig.1b. Another example of "magnetic fountain" with the different parameters: $k = (1Mm)^{-1}$, $Z(z) = 2(1+\exp(3kz))^{-1}$, $F^2 = 1+0.5\cdot Z\cdot abs(krJ_1(kr)\cdot\sin(20\varphi))$.

The images of "magnetic fountains with thin trickles" shown in Fig.1a,b are very similar to the pictures observed by Jafarzadeh et al (2017): "a dense forest of slender bright fibrils mapping the magnetic field…","loops are organized in canopy-like arches…". The pictures in Fig.1a,b are colored artificially in accordance with our calculations of T-profiles of the facular knots: their upper layers are hotter, than the lower.

After the substitution of corrected expression for (31) in (30), we obtain for the pressure in the knot the following expression (here we put for simplicity $G = 1$):

$$P(r,z,\varphi) =$$

$$= P_{ex}(z) + \frac{B_{ex}^2}{8\pi} - \frac{B_0^2 Z^2}{8\pi}\left[J_0^2\left(1 - \frac{Z''}{Z}\right) + \left(J_0^2 + \left(\frac{Z'}{Z}\right)^2\cdot J_1^2\right)\cdot f(r,\varphi,z) \right], \quad (35)$$

where $f(r,\varphi,z) = Z\cdot abs(krJ_1(kr)\cdot\sum_i a_i\sin(m_i\varphi))$.

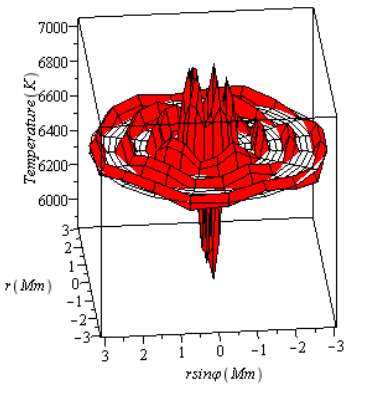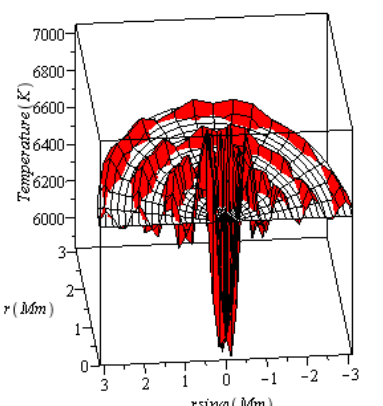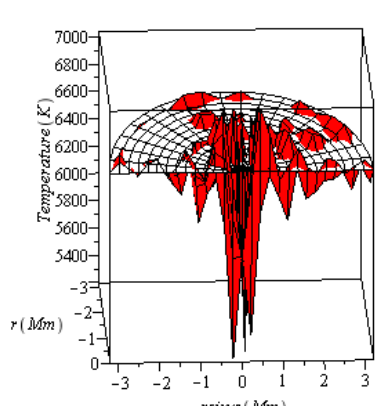For the density, the similar formula has the following form:

$$\rho(r,z) = \rho_{ex}(z) + \frac{B_0^2 k}{8\pi g} 2ZZ' \cdot \left[\left(1 - \frac{Z''}{Z}\right) \cdot J_1^2 + \left(1 - \frac{Z''}{2Z} - \frac{Z'''}{2Z'}\right) \cdot J_0^2 \right]. \quad (36)$$

Here the dash over Z indicates the derivative with respect to the argument of the exponent (kz).

5. Temperature profiles at different heights of atmosphere

In this Section we show the results of numerical calculations of temperature profiles for the facular knot defined by the formulae (33), (30), (4) and solar atmosphere model (Avrett & Loeser, 2008). We will calculate the function $T(r,\varphi)$ at different heights of the atmosphere, i.e. make a number of horizontal cross-sections of magnetic configurations shown in Fig.1a,b. These T-profiles will be calculated at the level of photosphere ($z = 0\ km$), temperature minimum ($z = 525\ km$), and at heights of $z = 1032\ km$, $z = 1520\ km$, $z = 2024\ km$ with the same value of inverse scale $k = 4\ (Mm)^{-1}$. For the angular coefficient m, we will take different values: from 0.5 to 50, and for the unit of magnetic field strength two values will be used: $B_0 = 1000\ G$, $B_0 = 500\ G$.

5.1. The base of the photosphere, z = 0. The temperature of plasma is 6583K

| Fig.2a. T-profile of the facula at $z = 0\ km$ for $B_0 = 1000\ G$, $m_1 = 15$, $m_2 = 10$, $a_1 = a_2 = 1$. Along the axis of the knot, the temperature drops below the photospheric value (white | Fig. 2b. The vertical cut of the same temperature profile. In this projection the central dip as well as the radial and the azimuthal variations of the temperature distribution are seen | Fig. 2c. The same configuration as in Fig. 2b, but the amplitudes of the function f is taken to be $a_1 = a_2 = 2$. As a result, the central depression is deepened, and the ring structures are |

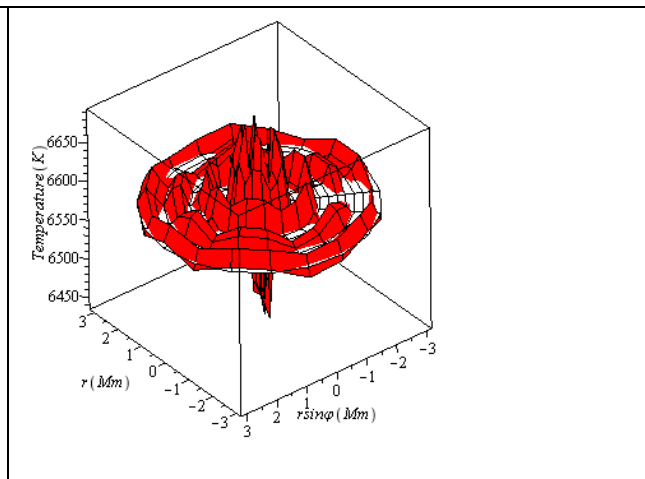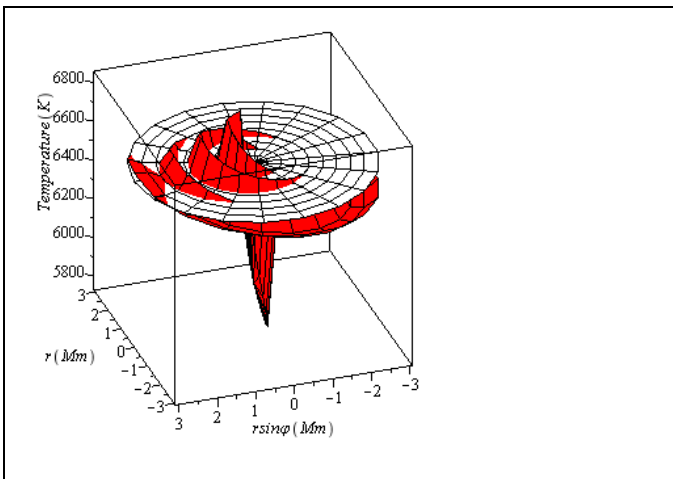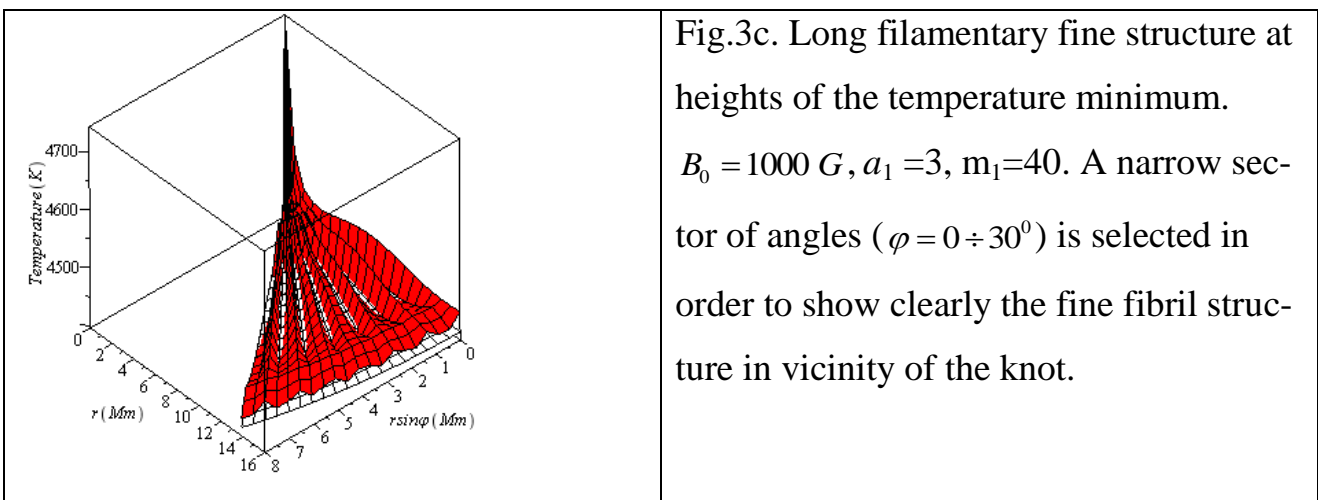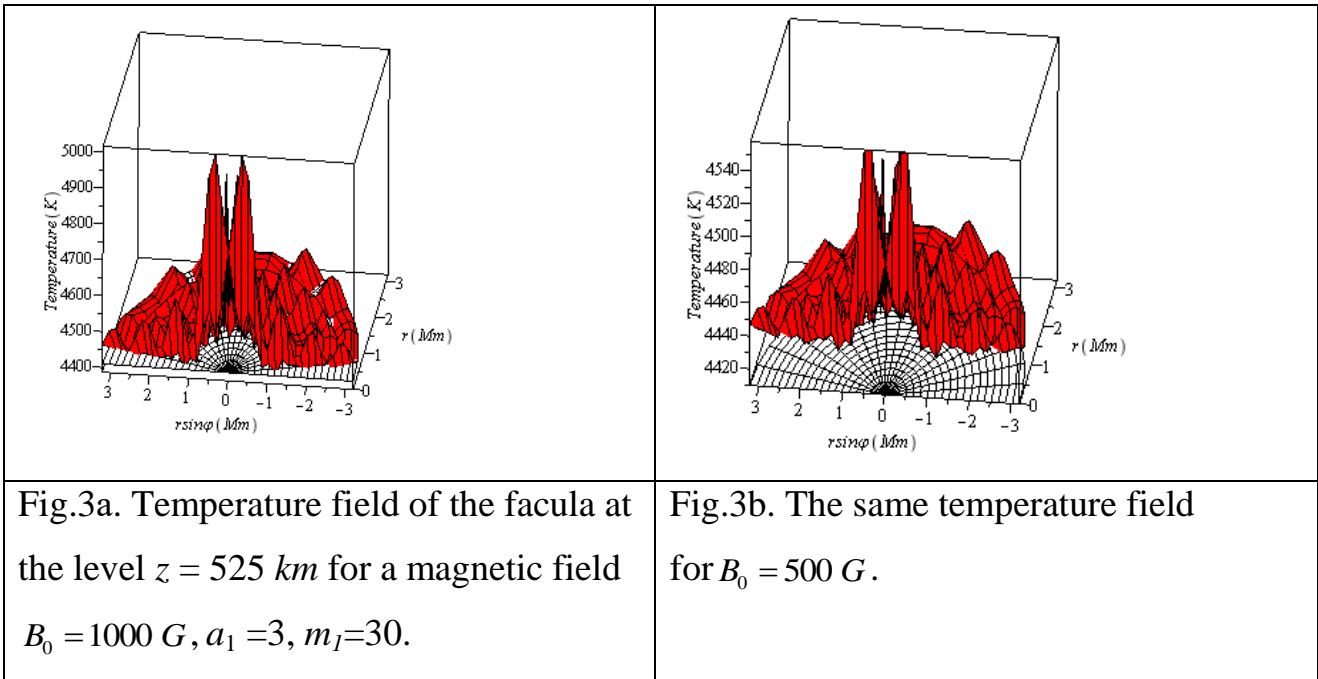| plane) by about 1200K (Wilson depression). The upper part of the knot is hotter the photosphere by the 250-300K.	clearly. White plane shows the temperature of the photosphere.	fragmented into separated "granules".

Fig.2d. Strong lateral asymmetry at the small value of angular parameter $m_1 = 0.5$, $m_2 = 0$, $a_1 = 2.5$, $a_2 = 0$. This image gives the impression that the magnetic flux tube is inclined to the left. Such phenomenon is often observed in the facular regions at high resolution: (Lites et al., 2004; Berger et al., 2007). Certainly, the magnetic flux tubes in facular regions can be really inclined, but in this case the visible effect is due to asymmetry of the temperature field.	Fig.2e. Temperature field of the facula at the level $z = 0\ km$ for a magnetic field twice smaller than the previous: $B_0 = 500\ G$. The amplitude of f is $a_1 = 1$, $a_2 = 1$ and $m_1 = 15$ and $m_2 = 10$. The T-profile conserves its geometrical form under a changing magnetic field strength but there is a respective reduction in the temperature range of the facular knot.

In all cases, at the level of photosphere there is a central dip in temperature profiles (similar to the Wilson's depression in sunspots), but a facular knot as a whole is hotter than the surrounding photosphere and therefore is clearly visible on the background of the photosphere. It is interested to note, that the photospheric T-profiles of

the facular knot are similar to usual torches that we use in the day to day life. They resemble a bright source with a cool handle which is used to hold the torch.

5.2. Low chromosphere. The temperature minimum (T = 4410К), z = 525 km.

Fig.3a. Temperature field of the facula at the level $z = 525$ km for a magnetic field $B_0 = 1000$ G, $a_1 = 3$, m_1=30.

Fig.3b. The same temperature field for $B_0 = 500$ G.

Fig.3c. Long filamentary fine structure at heights of the temperature minimum. $B_0 = 1000$ G, $a_1 = 3$, m$_1$=40. A narrow sector of angles ($\varphi = 0 \div 30^0$) is selected in order to show clearly the fine fibril structure in vicinity of the knot.

Here the temperature along the axis of faculae doesn't decrease strongly. The T-profiles of faculae as a whole are situated above the background and should be observed clearly at this height, the variation in temperature between lower and upper regions of the profile is about of 600K at the case of $B_0 = 1000$ G and about 100K with the $B_0 = 500$ G. We once again see that the geometrical form of the temperature profile doesn't change for large changes of the corresponding magnetic field strength, here only the temperature range changes.

In Fig.3c, a set of very long, slender and bright filaments is presented.

5.3. Level of z = 1003 km, the temperature of chromosphere is 6225К

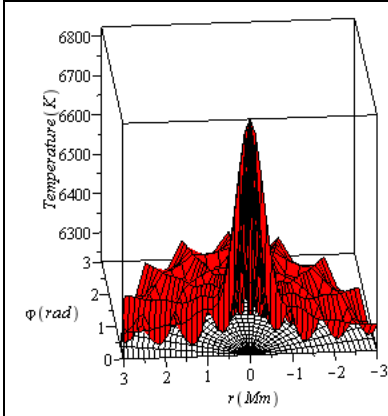Fig.4a. Temperature field of the facula at the level $z =1003$ km for a magnetic field $B_0 = 1000$ G. For the azimuthal number it is taken $m_1 = 40$, $a =3$.
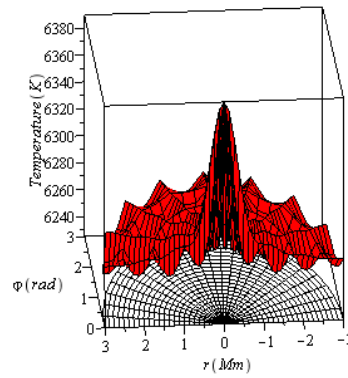

Рис.4b.Temperature field of the facula at the level z = 1003 km for a magnetic field twice smaller than the previous: $B_0 = 500$ G $m_1 = 40$, $a =3$.
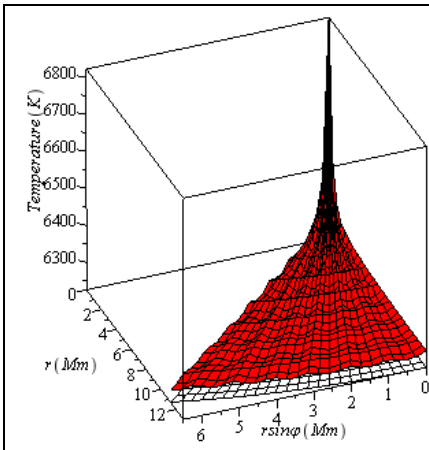

Fig.4c. At the height of 1003 km the fine filamentary structure of the field is already expressed to a much lesser extent. The same parameters as in Fig.3c: $B_0 = 1000$ G, $m_1 = 40$, $a =3$ are taken.

Here the temperature is large enough at the narrow central region of the faculae but the main body and periphery are slightly hotter than the surroundings.

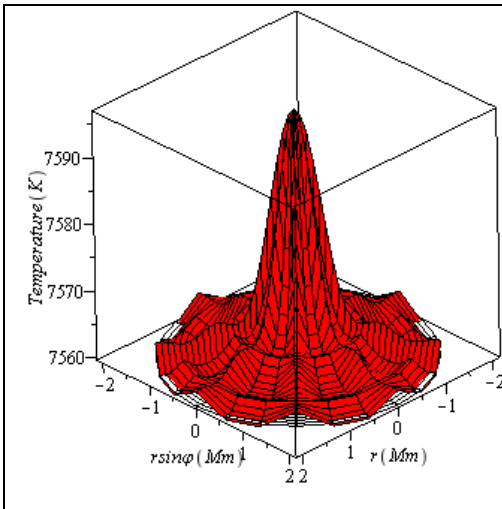### 5.4. Level with z = 1520 km, the temperature of chromosphere is 6623К.

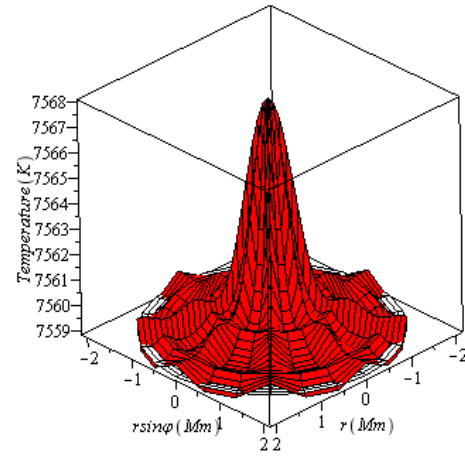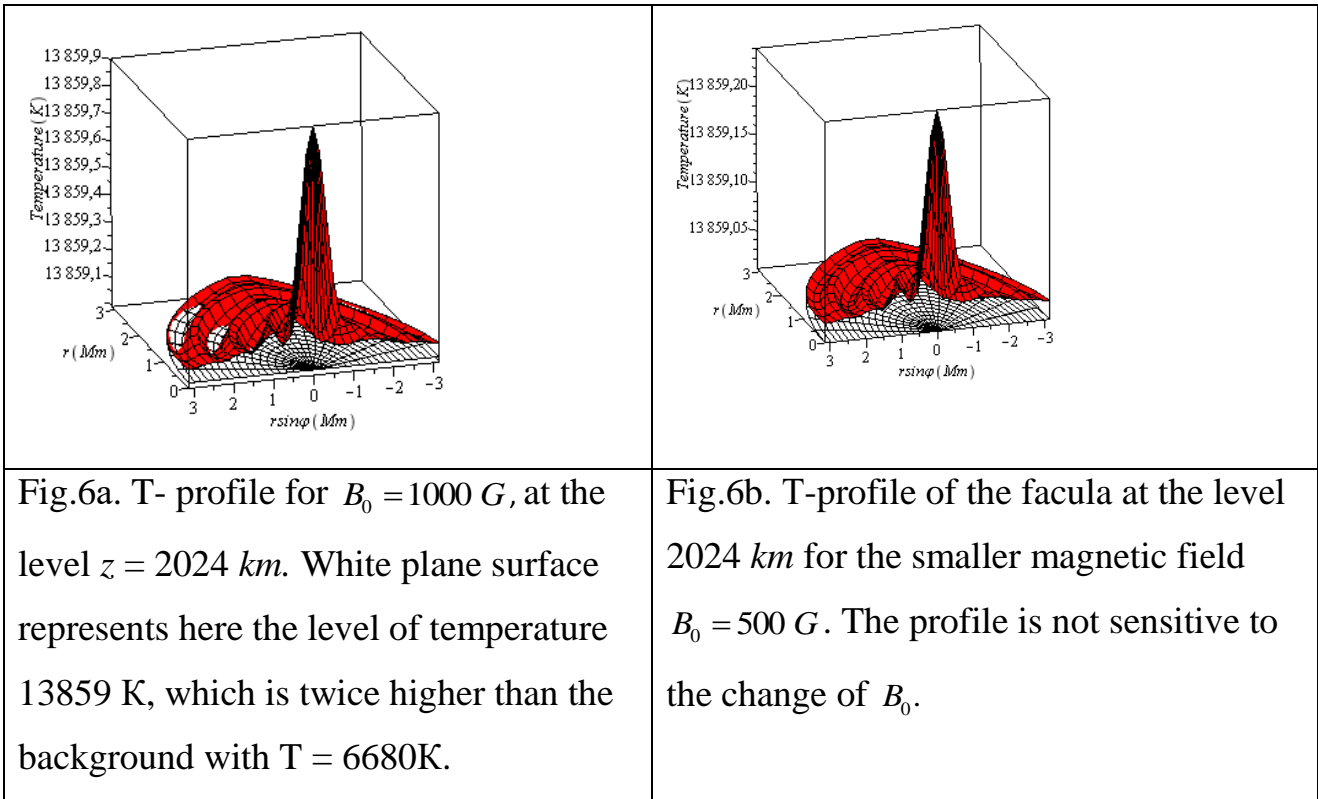|	
Fig. 5a. Temperature field of the facula at the level $z = 1520\ km$ for a magnetic field $B_0 = 1000\ G$, $m=20$, $a =3$.	Fig.5b. T-profile for the facula at the level $z = 1520\ km$ at $B_0 = 500\ G$. The range of temperature is decreased.

At these altitudes, the temperature in the central region of the faculae is high and the faculae as a whole appears to be hotter than the surroundings. Here the white plane surface doesn't represent the temperature of background that is 1000K lower than the average temperature of the facula. This plane represents only the temperature of the lowest layer of the faculae. Here the angular variation of the field doesn't play a noticeable role.

5.5. Level near the transition region, z = 2024 *km*, the temperature of the chromosphere is 6680K.

At the height of transition region we approach the boundary of the applicability of our model. Here the magnetic field in the flux tube becomes smaller than the external magnetic field, and the constant pressure of this external field $B_{ex}^2 (8\pi)^{-1} = 0.16\ dyn / cm^2$ gives the main contribution to the gas pressure of the facula. Therefore, as we see from Fig. 6ab, the temperature of the faculae markedly increases and ceases to depend on the field strength in the facular tube. Obviously, these results do not make sense in quantitative terms; they can only qualitatively indicate that the temperature of the facula somehow increases with height.

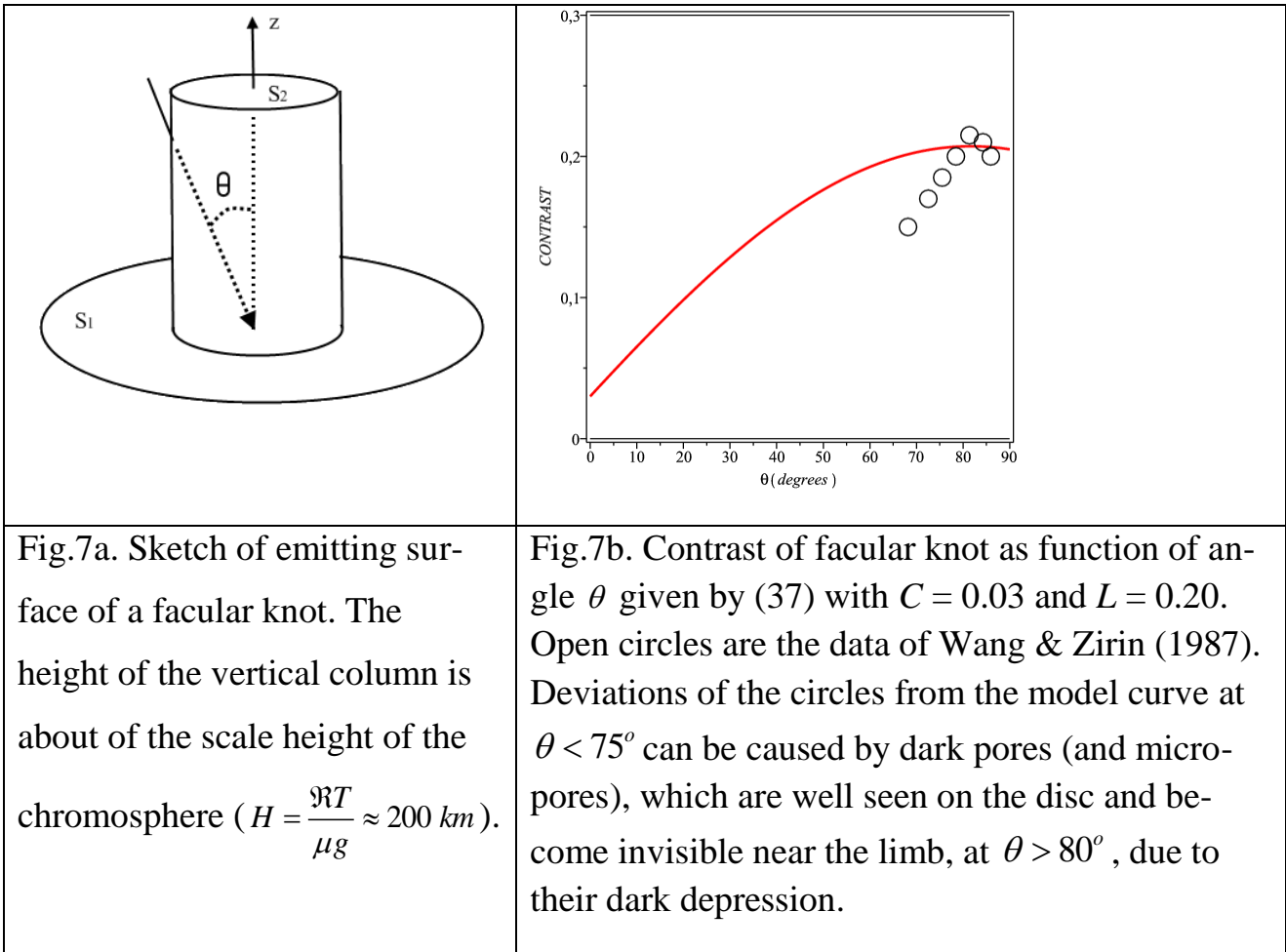| Fig.6a. T- profile for $B_0 = 1000\ G$, at the level $z = 2024\ km$. White plane surface represents here the level of temperature 13859 K, which is twice higher than the background with T = 6680K.	Fig.6b. T-profile of the facula at the level 2024 km for the smaller magnetic field $B_0 = 500\ G$. The profile is not sensitive to the change of B_0.

6. Center-to-Limb Variation Problem

The problem of brightness variations of faculae when they move along the solar disc is one of hard tasks of solar physics. The model of "hot walls" (Spruit, 1976) works satisfactorily on the disk, but it completely falls near the limb (Libbrecht & Kuhn,1984). In our model, according to the results above, we can present the emitting facular surfaces as a combination of a horizontal bases (S_1 and S_2) of the facula, with a temperature slightly above the background, and the bright lateral surface of a vertical cylinder (magnetic flux tube) (Fig.7a). The dependence of total contrast of such emitted configuration on the angle θ between the observer and the normal to the solar surface will be defined by following simple formula:

$$Contrast = \frac{\Delta I}{I} = C \cos \theta + L \sin \theta. \tag{37}$$

Here coefficients C and L are small positive numbers which should be searched on the base of observations. The coefficient C defines the contrast of faculae near the center of solar disc (about 0.03) and L gives the contrast of faculae at the limb (about 0.20). The corresponding curve is present in Fig.7b.

Fig.7a. Sketch of emitting surface of a facular knot. The height of the vertical column is about of the scale height of the chromosphere ($H = \dfrac{\Re T}{\mu g} \approx 200\ km$).	Fig.7b. Contrast of facular knot as function of angle θ given by (37) with $C = 0.03$ and $L = 0.20$. Open circles are the data of Wang & Zirin (1987). Deviations of the circles from the model curve at $\theta < 75^o$ can be caused by dark pores (and micropores), which are well seen on the disc and become invisible near the limb, at $\theta > 80^o$, due to their dark depression.

7. Conclusions

1.   A steady state 3D MHD model for the solar facular knot with fine filamentary structure of the magnetic field is constructed. Analytical formulae for the calculation of stationary distributions of gas pressure, density, Alfven Mach number and temperature according to the given magnetic configuration are derived.

2.   Facular magnetic configuration with external magnetic field of 2 *G* is introduced for the real solar atmosphere described by the Avrett & Loeser (2008) model.

3.   Numerically evaluated profiles of plasma temperature inside the facular knot at the level of the photosphere have the negative contrast at the axis (Wilson's depression), but at the nearest vicinities the temperature sharply rises and local rise in temperature of the individual facular granules above the surrounding medium is observed all along the area of the faculae. The geometry of T-profiles doesn't change even for large magnetic field variations. The variation of magnetic field only results in the change of the temperature range in the facula.

4. At the height of the temperature minimum (525 *km*), the entire profile of the faculae is located above the background and has temperature 1.2 times more that of the ambient plasma at this level.

5. At the heights of 1500 *km* above the photosphere, the gas of faculae is remarkable hotter than the ambient plasma at the same level. Most likely that due to the fact that faculae have a high temperature at the heights above 1 Mm, the observers distinguish between faculae and flocculi as two different phenomena. Faculae are considered to be photospheric and lower chromospheric phenomena and flocculi are considered to be the upper chromospheric phenomena.

6. In whole, the parameters and of the proposed model are in good correspondence with the most recent observational data of the solar faculae. This model in particular firstly describes the very fine filamentary arches-like structure of facular magnetic fields (magnetic "fountains" with the slender fibrils) as well as concentric rings, half rings and segmental brightening observed in the facular fields at high angular resolution at the photosphere level (Lites et al., 2004; Berger et al., 2007).

7. The new approach to the classic Center-to-Limb Variation Problem is proposed.

REFERENCES

Avrett E. H. & Loeser R., (2008). Models of the Solar Chromosphere and Transition Region from Sumer and HRTS Observations: Formation of the Extreme-Ultraviolet Spectrum of Hydrogen, Carbon and Oxygen. The Astrophysical Journal Supplement Series, 175: 229-276.

Baltasar H. (1990). The oscillatory behavior of solar faculae. Sol.Phys. **127**, 289-292.

Berger T.E., Rouppe L. van der Voort, Lofdahl M. (2007). Contrast analysis of solar faculae and magnetic bright points. Astrophys. J., **661,** 1272-1288.

Chelpanov, A.A., Kobanov, N.I., Kolobov, D.Y., (2015). Characteristics of oscillations in magnetic knots of solar faculae. Astron. Rep., **59**, 968-973.

Chapman G.A. & Klabunde D.P. (1982). Measurements of the limb darkening of faculae near solar limb. Astrophys.J. 261, 387-393

Jafarzadeh S., Rutten R.J., Solanki S.K. et al. (17 authors). (2017). Slender CAII H Fibrils Mapping Magnetic Field in the Low Solar Chromosphere. Astrophys. J. Supll. Ser. 229:11(11pp).

Kolotkov, D. Y., Smirnova, V. V., Strekalova, P. V., Riehokainen, A., Nakariakov, V. M. (2017). Long-period quasi-periodic oscillations of a small-scale magnetic structure on the Sun, Astronomy & Astrophysics, Vol. **598**, id. L2, 4 pp.

Kostik, R. & Khomenko, E.R. The possible origin of facular brightness in the solar atmosphere. Astronomy & Astrophysics„V. **589**, id.A6, 7 PP. (2016).

Libbrecht K.G.& Kuhn J.R. (1984) A new measurements of the facular contrast near the solar limb. Astrophys. J. 277, pp. 889-896.

Lites B. W., Scharmer G. B., Berger T. E. and Title A. M. (2004). Three-dimensional structure of the active region photosphere as revealed by high angular resolution. Solar Phys. **221**, 65-84.

Mehltretter J.P. (1974). Observations of photospheric faculae at the center of the solar disk. Solar Phys. **38**, 43-57.

Nakariakov, V.M., Aschwanden, M.J., & van Doorsselaere T. (2009).The possible role of vortex shedding in the excitation of kink-mode oscillations in the solar corona. Astronomy & Astrophysics, Vol. **502,** P. 661-664.

Okunev O.V., Kneer F. (2004). On the structure of polar faculae on the Sun. Astronomy & Astrophysics, Vol. 425**,** P. 321-331.

Pietarila, A.; Hirzberger, J.; Zakharov, V.; Solanki, S. K. (2009). Bright fibrils in Ca II K . Astronomy and Astrophysics, Vol. 502, pp.647-660.

Quintero Noda C.; Suematsu Y.; Cobo Ruiz B.;Shimizu T.; Asensio A. Ramos. (2016). Analysis of spatially deconvolved polar faculae. Monthly Notices of the Royal Astronomical Society, **460**, 956–965.

Shatten K.H., Mayr H.G., Omidrav K., Maier E. (1986). A hillock and cloud model for faculae. The Astrophysical Journal. **311.** 460-473.

Schatzman E. (1965). Model of a force free field. IAU Symp. **22**, Stellar and solar magnetic fields, Amsterdam, 337-345.

Scherrer P.H., Shou J., Bush R.I. et.al (13 authors), (2012) The Helioseismic and Magnetic Imager (HMI) Investigation for the Solar Dynamics Observatory (SDO), Solar Physics. Vol. 275, pp. 207-227. DOI: 10.1007/s11207-011-9834-2

Solov'ev A.A., Kirichek E.A. (2016). Analytical Model of an asymmetric sunspot with a steady plasma flow in its penumbra. Solar Physics.Vol. **291**, №6, 1647–1663.

Solov'ev A. A., Kirichek E.A. (2015). Magnetohydrostatics of a vertical flux tube in the solar atmosphere: coronal loops, a model of a ring flare filament. Astronomy Letters, vol.**41**, no.5, pp. 211-224. DOI: 10.1134/S1063773715050072).

Spruit H.C.(1976). Pressure equilibrium and energy balance of small photospheric flux tubes. Solar Phys.Vol.50, pp. 269-295.

Strekalova, P.V.; Nagovitsyn, Yu.A.; Riehokainen, A.; Smirnova, V.V. (2016).Long-period variations in the magnetic field of small-scale solar structures. Geomagnetism and Aeronomy, Vol. 56, Issue 8, pp.1052-1059.

Title A.M. & Schrijver C.J. (1998). The Sun's magnetic carpet. Cool stars, Stellar

Sytems and Sun. ASP Conf, Series. Vol.154, 345-358.

Title A.M., Topka K.P., Tarbell T.D. et al., (1992).On the differences between plage and quiet Sun in the solar photosphere. Astrophys. J. 393, 782-794.

Wang H. & Zirin H. (1987) The contrast of faculae near the solar limb. Solar Phys.110, 281-293.